Separation Science and Technology
Publication details, including instructions for authors and subscription information:
http://www.informaworld.com/smpp/title~content=t713708471

Removal of Actinides from Acidic Solution via Carrier-Mediated Facilitated Transport Across Mesoporous Substrates with Nanoengineered Surfaces: Thiol Self-Assembled Monolayers with D(tBu)ΦD(iBu)CMPO Ligands

K. Scott Sportsman[a]; Elizabeth A. Bluhm[a]; Kent D. Abney[a]
[a] Nuclear Materials Technology Division, Los Alamos National Laboratory, Los Alamos, NM, USA

To cite this Article Sportsman, K. Scott , Bluhm, Elizabeth A. and Abney, Kent D.(2005) 'Removal of Actinides from Acidic Solution via Carrier-Mediated Facilitated Transport Across Mesoporous Substrates with Nanoengineered Surfaces: Thiol Self-Assembled Monolayers with D(tBu)ΦD(iBu)CMPO Ligands', Separation Science and Technology, 40: 1, 709 — 723
To link to this Article: DOI: 10.1081/SS-200042676
URL: http://dx.doi.org/10.1081/SS-200042676

Separation Science and Technology, 40: 709–723, 2005
ISSN 0149-6395 print/1520-5754 online
DOI: 10.1081/SS-200042676

Removal of Actinides from Acidic Solution via Carrier-Mediated Facilitated Transport Across Mesoporous Substrates with Nanoengineered Surfaces: Thiol Self-Assembled Monolayers with D(tBu)ΦD(iBu)CMPO Ligands

K. Scott Sportsman, Elizabeth A. Bluhm, and Kent D. Abney
Nuclear Materials Technology Division, Los Alamos National Laboratory, Los Alamos, NM, USA

Abstract: The surface engineering of polycarbonate track-etched (PCTE) membranes was performed to create a permselective membrane for the removal of trace levels of fission products and transuranic metals from acidic streams. Electroless gold deposition was used to place a gold coating on the PCTE substrates. The gold coating was subsequently functionalized through the formation of a self-assembled monolayer of dodecanethiol, which was further functionalized with di-(4-t-butylphenyl)-N, N-diisobutylcarbamoylmethylphosphine oxide. Transport characteristics of metal ions, ^{137}Cs, ^{85}Sr, ^{241}Am, and ^{239}Pu, were obtained using a two-compartment diffusion apparatus. Transport studies showed that the functionalized membranes enhance the transport rates of ^{241}Am and ^{239}Pu and inhibit the transport of ^{137}Cs and

This work was funded by Paul Smith of NMT-2 through the Nuclear Material Stabilization Program, U.S. Department of Energy. The authors would also like to thank Keith Pannell, Department of Chemistry, University of Texas, El Paso, TX, and Louis D. Schulte, NMT-2, LANL, for providing the D(tBuΦ)D(iBu)CMPO ligand. Michael Cisneros of the Isotope and Nuclear Chemistry Group (C-INC), LANL, was invaluable to the authors in the preparation and purification of the radioisotopes that were used.

Address correspondence to K. Scott Sportsman, Nuclear Materials Technology Division, Los Alamos National Laboratory, Mail Stop E511, Los Alamos, NM 87545, USA. Tel: (505) 665-7021; E-mail: sport@lanl.gov

^{85}Sr. Diffusion studies over an extended time revealed that the facilitated transport characteristics of ^{239}Pu through the ligand-coated membranes are dependent on nitrate anion concentrations in the feed and sink cells.

INTRODUCTION

The TRansUranium EXtraction (TRUEX) process for the extraction of actinides is a heavily researched and accepted technology for recovery of actinides from acidic nuclear waste solutions. Liquid–liquid extraction is the primary unit operation in the TRUEX process, and the principal extractant for the removal of actinides is n-octyl(phenyl)-N,N-diisobutylcarbamoylmethylphosphine oxide (CMPO) (1). The TRUEX process is well suited for the recovery of actinides on a large scale; however, the required equipment, processing time and complexity, and vast quantities of the organic and rinse phases make this a prohibitive method for small-scale recovery of trace amounts of transuranic (TRU) metals. The Nuclear Materials Technology–Actinide Process Chemistry (NMT-2) group at Los Alamos National Laboratory (LANL) has developed a CMPO analog, di-(4-t-butylphenyl)-N,N,-diisobutylcarbamoylmethylphosphine oxide (D(tBuΦ)D(iBu)CMPO), to enhance the plutonium/americium separation efficiency and to maximize plutonium recovery. The molecular structures of both CMPO derivatives are shown in Fig. 1.

Chemical separations via membrane processes offer advantages over traditional separations technologies; membrane processes scale easily from bench top to process scale, they can reduce the separations' energy requirements, and they can be used to perform difficult separations (2, 3). Another appealing characteristic of membrane separations, particularly when compared to liquid–liquid extraction processes, is the reduction in the volume of the extractant phase.

Several studies have been performed utilizing supported liquid membranes (SLM), composed of CMPO dispersed in tributyl phosphate, to

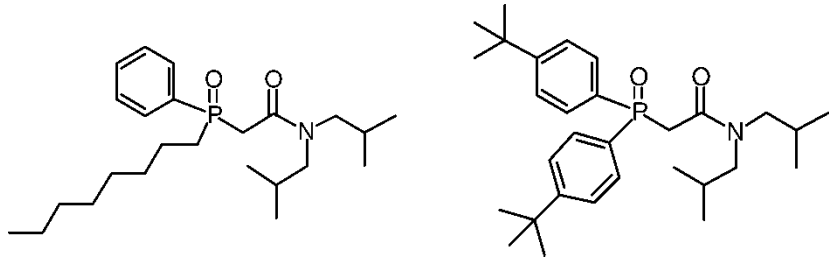

Figure 1. Molecular structure of (a) CMPO ligand used in TRUEX process and (b) D(tBuΦ)D(iBu)CMPO developed at LANL.

permeate trivalent actinide cations (4–6). These studies have shown that SLMs incorporating CMPO can successfully separate actinide cations from aqueous streams. CMPO also facilitates the transport of nitric acid across SLMs, although at a much lower rate than cations. However, stability is a weakness of the SLM approach.

While LANL has studied and utilizes numerous traditional separations operations, this research group has long had an interest in the use of membranes to perform actinide extractions. Previous work in this area has included the characterization of alumina membranes and their effect on cation transport (7, 8), the characterization of steel membranes for possible use as a substrate (9), the nanoengineering of a selective gate across the pore entrance of gold-sputtered alumina membranes (10), and the use of water soluble polymers to floc the metal ions preventing transport across ultrafiltration membranes (11, 12).

Each of these substrates, alumina and stainless steel, possesses undesired characteristics. The alumina substrates have high porosities with monodisperse pores, but the membranes are not stable in strong acids or bases. The stainless steel substrates also have very high porosities, but they have significantly larger membrane thicknesses, which, when combined with high tortuosities, adversely limit fluxes across the membranes. Recently, polycarbonate track-etched membranes (PCTE) have been investigated as an alternate substrate material.

PCTE membranes are well characterized, and their monodispersed, cylindrical pores have inspired significant interest in separations' research (13–19). Furthermore, PCTE membranes are easily coated with gold via an electroless gold-plating process (20–24). Treatment of gold surfaces with thiols results in self-assembled monolayers (SAMs) that can be used to functionalize the surface, allowing selective transport of a desired species (25–34), and also provides a method to increase the robustness of the membrane, when compared with SLMs.

Characterization studies of PCTE membranes have revealed that the nominal pore diameter should not be used without further characterization (31, 35, 36). While surface imaging studies suggest that the nominal pore diameters are accurate, hydraulic liquid permeation studies have revealed the effective diameters are significantly greater than the nominal values (13, 31, 35, 37, 38). Two mechanisms have been proposed to explain this anomaly.

The first is an apparent deformation of the membrane surface resulting from stress caused by the pressure drop across the membrane. Using membranes with a nominal pore diameter of 10 nm, a pressure drop of 100 kPa resulted in water fluxes corresponding to a pore diameter of 120 nm (35), while a pressure drop of 2 kPa resulted in an effective pore diameter of 24 nm (36). Previous studies by this research group confirmed that effective pore diameters of 26 nm were obtained with a pressure drop of $\sim$3 kPa using water and 18 nm using a mixture of isobutanol, methanol, and DI water (39).

A second explanation was derived from the use of PCTE membranes as templates to grow gold nanowires (31). Image analyses of the wires, following dissolution of the template, revealed that the pore diameters in the center of the membrane are two to three times larger than the pore diameters at the membrane surface. This cigar-shaped geometry results from secondary damage tracks along the primary track during manufacture.

EXPERIMENTAL

Materials

Poretics PCTE membranes (25 mm diameter, 6 μm thick, nominal 10 nm diameter pores, 6×10^8 pores cm^{-2}) were obtained from Osmonics, Inc. Oromorse SO Part B (a commercial gold-plating solution) was obtained from Technic Inc. ^{137}Cs radiotracer solution was obtained from Amersham Life Sciences with an activity of 5 mCi and a concentration of 0.1 mg/mL CsCl in 0.1 M HCl. ^{85}Sr (0.8 mL of 1.03 mCi/mL, Sr^{2+} in 0.1 M HCl) was obtained from the LANL Isotope Production and Distribution Program. ^{241}Am and ^{239}Pu radiotracers were obtained from stock solutions provided by LANL in 2 M HNO_3 solutions. The D(tBuΦ)D(iBu)CMPO ligands were prepared under contract by the Department of Chemistry, University of Texas, El Paso, TX. Deionized (DI) water (18 MΩ cm) from a Milli-Q Reverse Osmosis system (Millipore) was used to prepare all solutions. Reagent grade chemicals were obtained from Aldrich or Fisher Scientific and used as received.

Electroless Gold Deposition

Gold was deposited on both faces of the membranes and along the pore walls by electroless gold plating (20, 36). Following immersion in $AgNO_3$ solution, the PCTE membranes were rinsed in methanol and then immersed in the gold solution for 2 to 3 h. The temperature of the deposition solution was $\sim 2^{\circ}C$, and the pH was adjusted to 10. The gold-coated membranes were immersed in 25% nitric acid for ~10 to 12 h to clean the gold surface. Following the nitric acid treatment, the membranes were rinsed in DI water and then dried and stored in a desiccator under vacuum.

SAM Formation

Thiol chemisorption was used to form SAMs on the gold surfaces of the membranes. The chemisorption was performed by immersion of the

gold-treated membrane in an ethanol solution of 1 mM dodecanethiol (C_{12}) for 24 h. The membranes were then rinsed in ethanol for 1 h and dried under flowing N_2.

D(tBuΦ)D(iBu)CMPO molecules were adsorbed to the C_{12} SAM by immersion in a dodecane solution of the ligand ($\sim$1 M) for 24 h. The membranes were then rinsed in ethanol for 1 h and dried under N_2.

Following the gold-plating step, the SAM addition step, and the CMPO sorption step, the effective pore sizes were determined by measuring the flux of N_2 gas across the membranes resulting from an applied pressure drop (ΔP). For cylindrical pores, in which transport occurs by Knudsen diffusion, the gas flux (Q) through the membranes is related to the pore diameter (D) via Eq. (1) (40).

$$Q = \frac{1}{6}\left(\frac{2\pi}{MRT}\right)^{1/2}\left(\frac{\rho D^3}{l}\Delta P\right) \tag{1}$$

Nitrogen flux measurements across bare PCTE membranes with Eq. (1) yielded an effective pore diameter of 15.6 $\pm$ 0.67 nm.

Transport Experiments

Transport experiments were performed in two-compartment batch diffusion cells as shown in Fig. 2. Membranes were held in the vertical plane

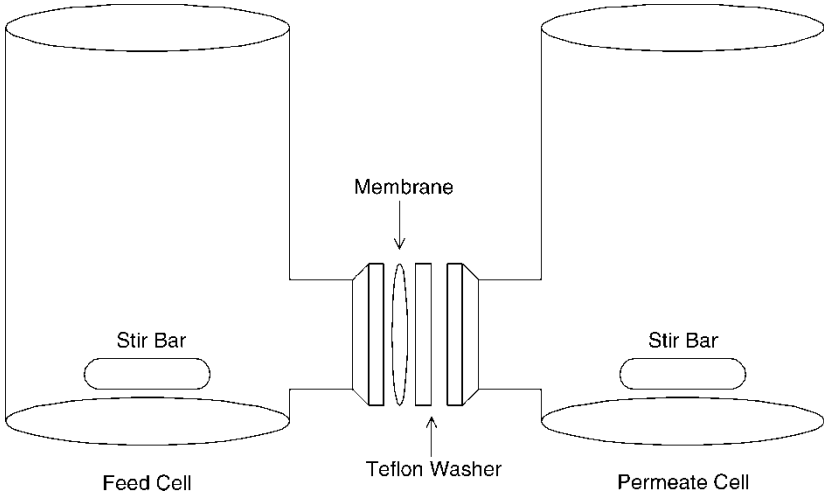

Figure 2. Schematic illustration of transport cells used in permeation studies. Liquid volume in each compartment is 100 mL, exposed membrane area is 3.1 cm^2 and stir speed is maintained at 300 rpm.

between the feed and sink cells by Viton O-rings and a Teflon washer. The effective permeation area of the membranes was 3.1 cm^2, and the feed and sink cell volumes were 100 mL. Stir rates were 300 rpm to minimize hydraulic boundary layers between the bulk solution and the membrane.

Similar procedures were followed for each transport experiment. Initially, the feed cells were filled with 100 mL of 7 M HNO_3, and the sink cells were filled with 100 mL of <0.1 M HNO_3. A brief observation period was used to detect leaks. If no leaks were observed, an aliquot (typically 100 μL) of radiotracer solution was added to the feed cell. The initial metal concentrations in the feed cells were 10^{-8} to 10^{-10} M. Transport across the membranes was monitored by periodically collecting 100 μL aliquots from the feed and sink cells. The ^{85}Sr and ^{137}Cs samples were diluted to 10 mL with DI water, and the isotope activities were counted using a Packard 500 NaI gamma counter. The ^{241}Am and ^{239}Pu aliquots were added to solutions containing 15 mL of Ultima Gold Alpha/Beta Scintillation Cocktail and 4.9 mL of DI water. Activities were measured on a Wallac 1414 scintillation counter. Metal ion concentrations were calculated from the measured activities using

$$C = \frac{A}{V_s \eta N_A \lambda} \tag{2}$$

The conditions of the feed and sink cells were determined from extraction chromatography studies using D(tBuΦ)D(iBu)CMPO (41). The distribution coefficients of Am(III) and Pu(IV) under these conditions are given in Table 1.

The relationship between the radionuclide concentrations and permeability coefficients can be determined by a mass balance between the feed and sink cells.

$$\ln\left[\frac{[C_{i,f}]}{[C_{i,f}]_o}\right] = -\left(\frac{S\varepsilon}{V}\right)P_i t \tag{3}$$

Table 1. Distribution coefficients (K_d) of Am(III) and Pu(IV) with D(tBuΦ)D(iBu)CMPO (41)

$[NO_3^-]$	Am(III)	Pu(IV)
0.1	110	< 150
3	9000	30000
7	10000	10000

RESULTS

Gas Flux Measurements

Figure 3 shows the relationship between the effective pore diameter and the plating time, as determined by N_2 fluxes following the electroless gold-plating procedure. The error bars represent one standard deviation from at least three replicate measurements. The discontinuity occurring after a plating time of 4 h is likely the result of a transition from Knudsen diffusion to a frictional flow mechanism as the pore size approaches the mean free path length of the N_2 molecules. The membranes used in this study were subjected to 2 to 3 h plating periods resulting in pore diameters of 5 to 6 nm.

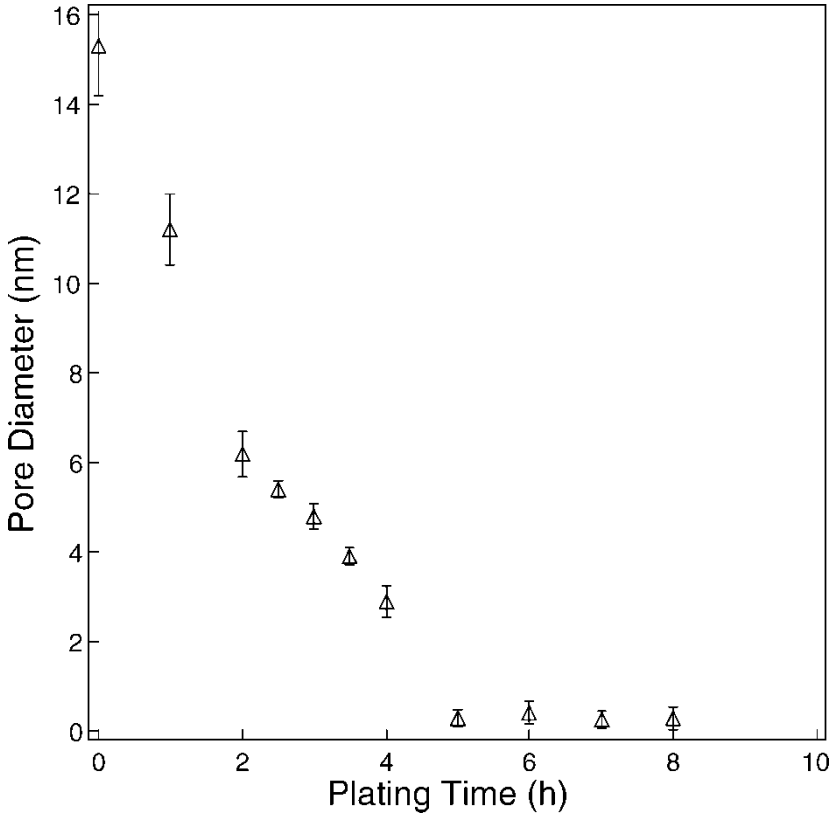

Figure 3. Electroless plating rate as determined by N_2 gas permeation measurements.

The gas flux measurements following the addition of the SAMs did not statistically differ from the measurements following the gold-plating step. This indicates that the change in pore diameter resulting from the SAM was below the sensitivity of the gas permeation apparatus. However, the efficacy of the SAM procedure becomes apparent from the metal ion transport results.

Metal Transport Results

Metal ion transport studies were conducted for each metal through untreated PCTE membranes, gold-coated membranes, membranes with C_{12} SAMs, and membranes coated with D(tBuΦ)D(iBu)CMPO. Figure 4 shows the concentration of Cs^+ ions in the sink normalized by the initial concentration of Cs^+ in the feed. Permeant flux, which can be obtained from the slope of concentration/time plots as given in Eq. (4), decreases as the pore size is reduced via the electroless gold-plating process.

$$J = \frac{4}{\pi}\frac{\mathrm{VS}\rho}{\mathrm{D}^2}\frac{\mathrm{dC}}{\mathrm{dt}} \tag{4}$$

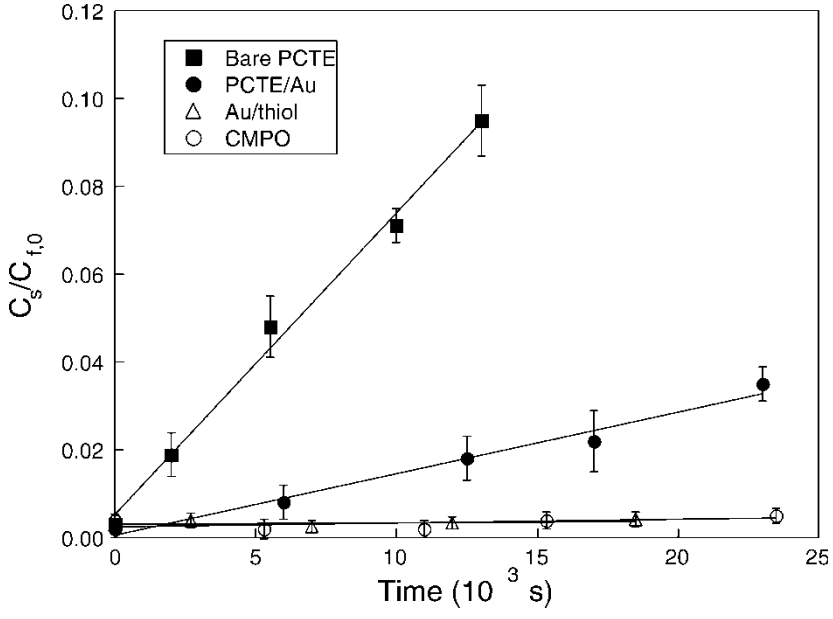

Figure 4. Diffusion of ^{137}Cs across PCTE, PCTE/Au, PCTE/Au/thiol, and PCTE/Au/thiol/CMPO membranes. Concentrations of ^{137}Cs in the sink normalized by the initial concentration in the feed cell.

During the experiments, flux rates decrease as the concentration difference between the feed and sink decreases, until the chemical potentials across the membrane, resulting from the difference in concentration, are equal. The C_{12} SAM prevents diffusion of the Cs^+ ions across the membrane, and Cs^+ diffusion remains negligible following the addition of D(tBuΦ)D(iBu)CMPO. Similar results were observed with Sr^{2+}; pore size reduction decreases the flux, and functionalization prevents diffusion across the membranes.

These results can be used to further characterize the surface nanoengineering effort. The diffusion results reflect the decrease in pore size by the gold layer and suggest that the SAM may have occluded the pores. The Cs^+ and Sr^{2+} diffusion results do not indicate a change in membrane properties with the addition of D(tBuΦ)D(iBu)CMPO. Nitrogen gas permeation data also reflect the reduction in pore size from the electroless gold-plating process but does not indicate a change in pore size from the SAM, which was expected to reduce the pore diameter by $\sim$2 nm. Thus, the decrease in flux of Cs^+ and Sr^{2+} through SAM-treated membranes can be attributed to changes in the pore walls' chemical characteristics. The C_{12} coating introduces a hydrophobic characteristic, resulting in the loss of fluxes.

Figure 5 shows normalized sink concentrations of Am(III) through each of the membrane surface types. As with Cs^+ and Sr^{2+}, the decrease in pore

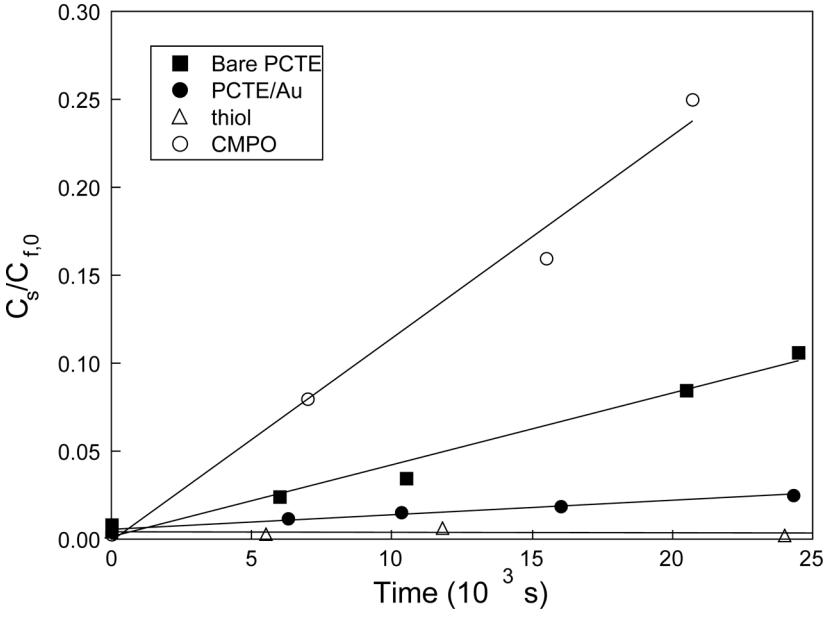

Figure 5. Change in ^{241}Am sink cell concentration, normalized by the initial feed concentration by diffusion across membranes with different surfaces.

diameter, resulting from addition of the gold layer, significantly decreases the flux of Am(III) across the membrane. Additionally, the presence of the thiol SAM prevents the diffusion of Am(III). However, a significant change occurs with the addition of D(tBuΦ)D(iBu)CMPO. Unlike Cs^{+} and Sr^{2+}, Am(III) flux across the membrane increases with the addition of D(tBuΦ) D-(iBu)CMPO. Furthermore, the presence of the ligand results in quantitative transport of Am(III) from the feed reservoir to the sink, indicating that D(tBuΦ)-D(iBu)CMPO molecules are carriers in the facilitated transport of Am(III).

Material balances following the D(tBuΦ)D(iBu)CMPO Am(III) transport experiments reveal a significant (~20%) loss of total activity from the feed and sink cells. Previous experiments typically had activity losses of <3% of the total activity, which was attributed to sampling/counting error and negligible hold up of metal ions within the membranes. The greater activity loss of the Am(III) studies is attributed to the coordination properties between the D(tBuΦ)D(ibu)CMPO ligand and trivalent actinides. Desorption caused by the low nitrate concentration in the sink cells is an equilibrium process; and although the K_d is much lower at $[NO_3^-] < 0.1$, there is still a thermodynamic distribution between the solid membrane/ligand phase and the aqueous phase, resulting in incomplete desorption from the membrane.

Diffusion of Pu(IV) across the membranes is shown in Fig. 6. These results are similar to those of the Am(III) studies, including the loss of

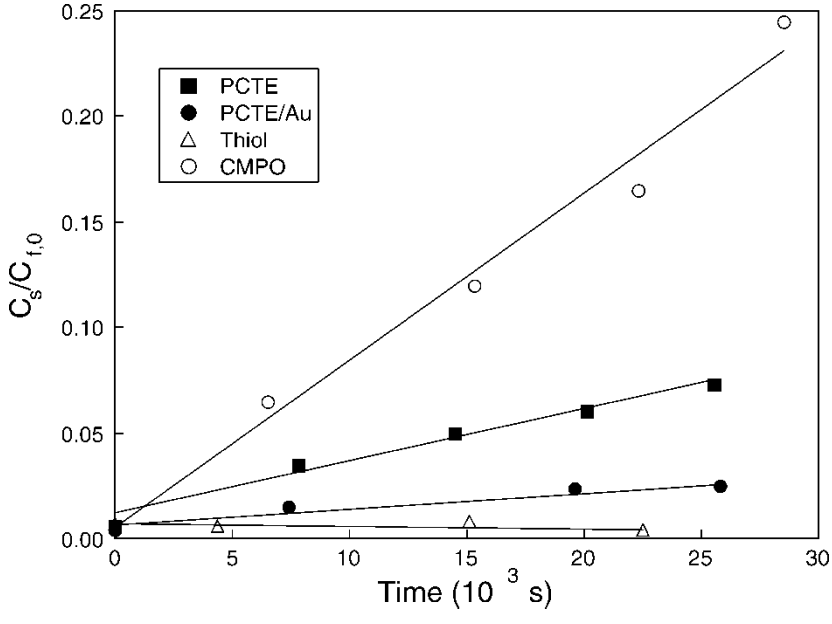

Figure 6. Change in ^{239}Pu concentration in the sink cell across membranes during various steps of the surface engineering process.

$\sim$23% of the initial activity. Pu(IV) was also actively transported across the membrane, resulting in a nearly complete removal of Pu(IV) from the feed cell. The transport mechanism was further investigated through extended time diffusion experiments, the results of which are shown in Fig. 7. Pu(IV) is transported from the feed cell to the sink cell in 40 h, at which time transport appears to cease. However, by extending the sampling period, an apparent reversal in transport is observed; the Pu(IV) activity in the sink cell decreases. By the end of the experimental run, approximately 1 week, the total measurable activity in the feed and sink cells had decreased from $\sim$1400 to $\sim$150 cpm.

The change in transport behavior results from the low rate of nitric acid transport across the membranes. During the short transport studies, changes in the feed and sink cell nitric acid concentrations were negligible; however, by extending the time studied, the nitric acid concentration of the sink cell increases. At high nitric acid concentrations, CMPO molecules coordinate with plutonium/nitrate complexes and extract them from the acid stream into the organic stream. Pu is then removed from the CMPO coordination by the low nitric acid concentration of the bulk solution, which strips the nitrate anions from the Pu(IV)/nitrate/CMPO complex. Initially, the nitric acid concentration in the feed was 7.1 M, and Pu(IV) transport

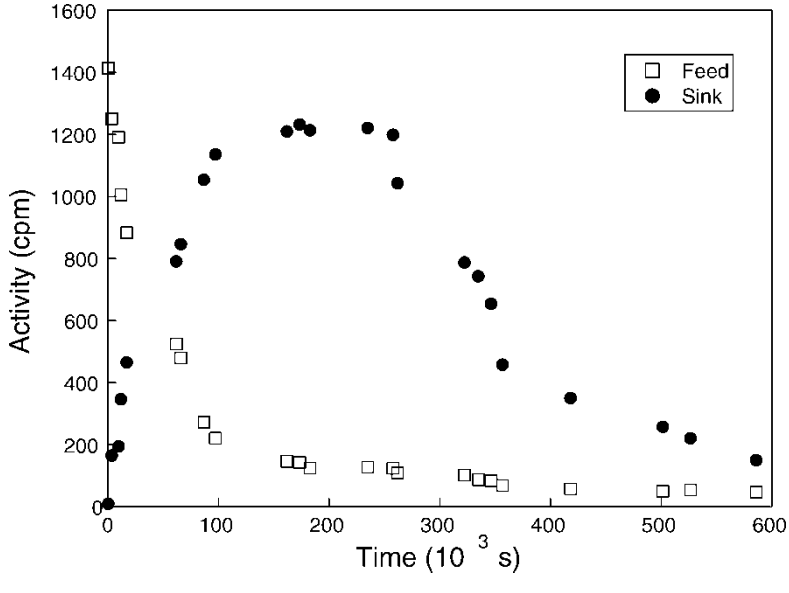

Figure 7. Change in ^{239}Pu concentrations in the feed and sink cells during a transport experiment continued for an extended time period.

occurred from the feed cell to the sink cell. As nitric acid diffuses across the membrane, $[NO_3^-]_{sink}$ increases, and the equilibrium conditions between the D(tBuΦ)D(iBu)CMPO ligands in the membrane and the bulk solutions undergo significant changes favoring the sorption of Pu(IV) from both the feed and sink cell into the membrane. The loss of activity in the feed and sink cell is due to the greater distribution coefficient at higher nitric acid concentrations, as shown in Table 1.

CONCLUSIONS

These studies have shown that transport properties of mesoporous PCTE membranes can be modified through surface engineering. As described by Hagen-Poisseuille's equation for laminar flow through a cylinder, reduction of pore diameter, via electroless gold plating, results in the decrease of diffusional flux across the membranes, with a similar order of magnitude reduction occurring for each of the metal ions studied, ^{137}Cs, ^{85}Sr, ^{241}Am, and ^{239}Pu. Following gold deposition on the PCTE substrate, a dodecanethiol SAM was added. Although the SAM did not significantly reduce the pore diameter, the hydrophobic nature of the thiol significantly increased the transport resistance of the membrane, essentially preventing any of the metals from diffusing across the membrane. The final step in the surface modification was the addition of the D(tBuΦ)D(ibu)CMPO ligand to the PCTE/Au/SAM membranes. The monovalent and divalent cations were still unable to diffuse across the membranes, but the trivalent and tetravalent actinides were quantitatively extracted from the feed cell to the sink cell through a carrier-mediated, facilitated transport mechanism. Furthermore, the flux rates of the actinides across the membranes were much greater than the flux rates across the bare PCTE membranes or the PCTE/Au membranes. However, the desorption mechanism into the sink solution under the experimental conditions was imperfect, causing a loss of 20 to 25% of the total activity from the experiments. Additionally, by extending the time of the diffusion experiments, the conditions of the feed and sink cells, in particular nitrate anion concentrations, were allowed to change. As the nitrate concentration in the sink cell increased, Pu(IV) was sorbed from the sink into the membrane, resulting in a near total loss of activity.

These results indicate that the carrier-mediated, facilitated transport approach is a promising method of removing low levels of actinides from process streams, while not generating copious amounts of secondary wastes. Operationally, the transient change in nitrate anion concentration could be easily avoided by recirculating the contents in the sink cell, by removing HNO_3 from the sink to prevent accumulation, or by binding the Pu in the sink with oxalate or other complexants.

NOMENCLATURE

A	Activity of radionuclide
C	Concentration of radionuclide
$C_{i,f}$	Concentration of species i in the feed (subscript o denotes initial concentration)
D	Pore diameter
J	Flux of radionuclide
l	Membrane thickness
M	Molecular weight of permeating gas
N_A	Avogadro's number
P_i	Permeability coefficient of species i
ΔP	Pressure drop across membrane
Q	Volumetric water flux
R	Gas constant
S	Membrane area
t	Time
T	Temperature
V	Volume of sink or feed solution
V_s	Volume of sample aliquot
η	Counter efficiency
ρ	Pore density
ε	Porosity
λ	Decay constant

REFERENCES

1. Mathur, J.N., Murali, M.S., and Nash, K.L. (2001) Actinide Partitioning: A Review. *Solvent Extr. Ion Exch.*, 19: 357–390.
2. Drioli, E. and Romano, M. (2001) Progress and New Perspectives on Integrated Membrane Operations for Sustainable Industrial Growth. *Ind. Eng. Chem. Res.*, 40: 1277–1300.
3. Mulder, M.H.V. (1996*Basic Principles of Membrane Technology*, 2nd Ed.; Kluwer Academic Publishers: Dordrecht, Netherlands.
4. Chiarizia, R. and Danesi, P. (1987) A Double Liquid Membrane System for the Removal of Actinides and Lanthanides from Acidic Nuclear Wastes. *Sep. Sci. Technol.*, 22: 641–659.
5. Danesi, P. and Cianetti, C. (1984) Permeation of Metal-Ions Through a Series of 2 Complementary Supported Liquid Membranes. *J. Membr. Sci.*, 20: 201–213.
6. Danesi, P., Chiarizia, R., Rickert, P., and Horwitz, E. (1985) Separation of Actinides and Lanthanides from Acidic Nuclear Wastes by Supported Liquid Membranes. *Solvent Extr. Ion Exch.*, 3: 111–147.
7. Bluhm, E.A., Bauer, E., Chamberlin, R.M., Abney, K.D., Young, J.S., and Jarvinen, G.D. (1999) Surface Effects on Cation Transport Across Porous Alumina Membranes. *Langmuir*, 15: 8668–8672.

8. Bluhm, E.A., Schroeder, N.C., Bauer, E., Fife, J.N., Chamberlin, R.M., Abney, K.D., Young, J.S., and Jarvinen, G.D. (2000) Surface Effects on Metal Ion Transport Across Porous Alumina Membranes. 2. Trivalent Cations: Am; Tb; Eu; and Fe. *Langmuir*, 16: 7056–7060.
9. Ames, R.L., Bluhm, E.A., Way, J.D., Bune, A.L., Abney, K.D., and Schreiber, S.B. (2003) Physical Characterization of 0.5 μm Cut-Off Sintered Stainless Steel Membranes. *J. Membr. Sci.*, 213: 13–23.
10. Mccleskey, T.M., Ehler, D.S., Young, J.S., Pesiri, D.R., Jarvinen, G.D., and Sauer, N.N. (2002) Asymmetric Membranes with Modified Gold Films as Selective Gates for Metal Ion Separations. *J. Membr. Sci.*, 210: 273–278.
11. Barr, M.E., Schulte, L.D., Jarvinen, G.D., Espinoza, J., Ricketts, T.E., Valdez, Y., Abney, K.D., and Bartsch, R.A. (2001) Americium Separations from Nitric Acid Process Effluent Streams. *J. Radioanal. Nucl. Chem.*, 248: 457–465.
12. Barr, M.E., Jarvinen, G.D., Moody, E.W., Vaughn, R., Silks, L.A., and Bartsch, R.A. (2002) Plutonium(iv) Sorption by Soluble Anion-Exchange Polymers. *Sep. Sci. Technol.*, 37: 1065–1078.
13. Apel, P. (2001) Track Etching Technique in Membrane Technology. *Radiat. Meas.*, 34: 559–566.
14. Chen, S.H., Ruaan, R.C., and Lai, J.Y. (1997) Sorption and Transport Mechanism of Gases in Polycarbonate Membranes. *J. Membr. Sci.*, 134: 143–150.
15. Fang, Y. and Leddy, J. (1995) Surface-Diffusion in Microstructured; Ion-Exchange Matrices: Nafion/Neutron Track-Etched Polycarbonate Membrane Composites. *J. Phys. Chem.*, 99: 6064–6073.
16. Kuo, T.C., Cannon, D.M., Shannon, M.A., Bohn, P.W., and Sweedler, J.V. (2003) Hybrid Three-Dimensional Nanofluidic/Microfluidic Devices Using Molecular Gates. *Sens. Actuators, A*, 1: 223–233.
17. Macpherson, J.V., Jones, C.E., Barker, A.L., and Unwin, P.R. (2002) Electrochemical Imaging of Diffusion Through Single Nanoscale Pores. *Anal. Chem.*, 15: 1841–1848.
18. Martinez, L., Tejerina, A.F., and Arribas, J.I. (1987) Diffusion of LiCl Through Nuclepore Membranes of Polycarbonate. *J. Non-Equilib. Thermodyn.*, 12: 245–253.
19. Shao, J.H. and Baltus, R.E. (2000) Effect of Solute Concentration on Hindered Diffusion in Porous Membranes. *AIChE J.*, 46: 1307–1316.
20. Menon, V.P. and Martin, C.R. (1995) Fabrication and Evaluation of Nanoelectrode Ensembles. *Anal. Chem.*, 67: 1920–1928.
21. Nishizawa, M., Menon, V.P., and Martin, C.R. (1995) Metal Nanotubule Membranes with Electrochemically Switchable Ion-Transport Selectivity. *Science*, 268: 700–702.
22. Jirage, K.B., Hulteen, J.C., and Martin, C.R. (1997) Nanotubule-Based Molecular-Filtration Membranes. *Science*, 278: 655–658.
23. Wirtz, M., Yu, S.F., and Martin, C.R. (2002) Template Synthesized Gold Nanotube Membranes for Chemical Separations and Sensing. *Analyst*, 127: 871–879.
24. Wirtz, M., Parker, M., Kobayashi, Y., and Martin, C.R. (2002) Template-Synthesized Nanotubes for Chemical Separations and Analysis. *Chem. Eur. J.*, 16: 3573–3578.
25. Ulman, A. (1996) Formation and Structure of Self-Assembled Monolayers. *Chem. Rev.*, 96: 1533–1554.

26. Feldheim, D.L., Lawson, D.R., and Martin, C.R. (1993) Influence of the Sulfonate Countercation on the Thermal-stability of Nafion(r) Perfluorosulfonate Membranes. *J. Polym. Sci., Part B: Polym. Phys.*, 31: 953–957.
27. Hou, Z.Z., Abbott, N.L., and Stroeve, P. (1998) Electroless Gold as a Substrate for Self-Assembled Monolayers. *Langmuir*, 14: 3287–3297.
28. Hulteen, J.C., Jirage, K.B., and Martin, C.R. (1998) Introducing Chemical Transport Selectivity into Gold Nanotubule Membranes. *J. Amer. Chem. Soc.*, 120: 6603–6604.
29. Hou, Z.Z., Dante, S., Abbott, N.L., and Stroeve, P. (1999) Self-Assembled Monolayers on (111) Textured Electroless Gold. *Langmuir*, 15: 3011–3014.
30. Jirage, K.B., Hulteen, J.C., and Martin, C.R. (1999) Effect of Thiol chemisorption on the Transport Properties of Gold Nanotubule Membranes. *Anal. Chem.*, 71: 4913–4918.
31. Martin, C.R., Nishizawa, M., Jirage, K., and Kang, M. (2001) Investigations of the Transport Properties of Gold Nanotubule Membranes. *J. Phys. Chem. B*, 105: 1925–1934.
32. Chun, K.Y. and Stroeve, P. (2002) Protein Transport in Nanoporous Membranes Modified with Self-Assembled Monolayers of Functionalized Thiols. *Langmuir*, 18: 4653–4658.
33. Vericat, C., Andreasen, G., Vela, M.E., Martin, H., and Salvarezza, R.C. (2001) Following Transformation in Self-Assembled Alkanethiol Monolayers on Au(111) by In Situ Scanning Tunneling Microscopy. *J. Chem. Phys.*, 8: 6672–6678.
34. Casero, E., Darder, M., Pariente, F., Lorenzo, E., Martin-Benito, J., and Vazquez, L. (2002) Thiol-Functionalized Gold Surfaces as a Strategy to Induce Order in Membrane-Bound Enzyme Immobilization. *Nano Lett.*, 2: 577–582.
35. Kim, K.J. and Stevens, P.V. (1997) Hydraulic and Surface Characteristics of Membranes with Parallel Cylindrical Pores. *J. Membr. Sci.*, 123: 303–314.
36. Hou, Z.Z., Abbott, N.L., and Stroeve, P. (2000) Self-Assembled Monolayers on Electroless Gold Impart pH-Responsive Transport of Ions in Porous Membranes. *Langmuir*, 16: 2401–2404.
37. Pandey, A.K., Gautam, M.M., Shukla, J.P., and Iyer, R.H. (2001) Effect of Pore Characteristics on Carrier-Facilitated Transport of Am(III) Across Track-Etched Membranes. *J. Membr. Sci.*, 190: 9–20.
38. Calvo, J.I., Hernandez, A., Caruana, G., and Martinez, L. (1995) Pore-Size Distributions in Microporous Membranes. 1. Surface Study of Track-Etched Filters by Image-Analysis. *J. Colloid Interface. Sci.*, 175: 138–150.
39. Sportsman, K.S., Bluhm, E.A., and Abney, K.D. (2004) Pore Effects on Cation Transport Across PCTE Membranes. *J. Membr. Sci.* (submitted).
40. Petzny, W.J. and Quinn, J.A. (1969) Calibrated Membranes with Coated Pore Walls. *Science*, 166: 751–753.
41. Abney, K.D., Cisneros, M.R., Pearce, R., Mahar, M.M., Kersey, S.J., and Schulte, L.D. (2001*Plutonium Decontamination of Nitric Acid Process Effluents Using Extraction Chromatography*; Los Alamos National Laboratory: Los Alamos, New Mexico; LAUR-01-1679.